HHS Public Access

Author manuscript

J Biomech. Author manuscript; available in PMC 2016 March 08.

Published in final edited form as:

J Biomech. 2014 January 22; 47(2): 392–399. doi:10.1016/j.jbiomech.2013.11.015.

Analysis of the musculoskeletal loading of the thumb during pipetting – A pilot study

John Z. Wu[a,*], **Erik W. Sinsel**[a], **Justin F. Shroyer**[a], **Christopher M. Warren**[a], **Daniel E. Welcome**[a], **Kristin D. Zhao**[b], **Kai-Nan An**[b], and **Frank L. Buczek**[a]

[a]National Institute for Occupational Safety & Health, Morgantown, WV 26505, USA

[b]Biomechanics Laboratory, Division of Orthopedic Research, Mayo Clinic, Rochester, MN 55905, USA

Abstract

Previous epidemiological studies indicate that the use of thumb-push mechanical pipettes is associated with musculoskeletal disorders (MSDs) in the hand. The goal of the current study was to analyze the loading in the muscle–tendon units in the thumb during pipetting. The hand is modeled as a multi-body linkage system and includes four fingers (index, long, ring, and little finger), a thumb, and a palm segment. Since the current study is focused on the thumb, the model includes only nine muscles attached to the thumb via tendons. The time-histories of joint angles and push force at the pipette plunger during pipetting were determined experimentally and used as model input; whereas forces in the muscle–tendon units in the thumb were calculated via an inverse dynamic approach combined with an optimization procedure. Results indicate that all nine muscles have force outputs during pipetting, and the maximal force was in the abductor pollicis brevis (APB). The ratio of the mean peak muscle force to the mean peak push force during the dispensing cycle was approximately 2.3, which is comparable to values observed in grasping tasks in the literature. The analysis method and results in the current study provide a mechanistic understanding of MSD risk factors associated with pipetting, and may be useful in guiding ergonomic designs for manual pipettes.

Keywords

Thumb; Muscle–tendon force; Pipette; Modeling; Inverse dynamics

1. Introduction

Highly repetitive manual work is associated with the development of upper extremity musculoskeletal disorders (MSDs) (Barr et al., 2004; Muggleton et al., 1999; Ranney et al.,

*Correspondence to: NIOSH/CDC, 1095 Willowdale Road, MS-2027, Morgantown, WV 26505, USA. Tel.: +1 304 285 6265; fax: +1 304 285 5832. jwu@cdc.gov (J.Z. Wu)..

Conflict of interest statement All authors of this paper have no conflict of interest.

1995), with tendinitis being one of the most common syndromes in upper extremity MSDs (Wainstein and Nailor, 2006). The risk of tendinitis in workers who perform highly repetitive forceful jobs is 29 times greater than those who perform jobs that are low in repetitions and force (Armstrong et al., 1987). Manual pipetting involves repetitive motion of the thumb for extracting and dispensing fluids, during which the muscles/tendons and articular joints of the thumb, hand and wrist are exposed to highly repetitive motion and loading. A survey-based study (David and Buckle, 1997) showed that almost 90% of pipette users, who continuously use pipettes for more than an hour on a daily basis, reported hand and/or elbow disorders. Further, some pipette users complain of discomfort not only in the thumb, wrist, and elbow (Baker and Cooper, 1998; Heath, 1998), but also in the shoulder and neck (David and Buckle, 1997; McKean et al., 2005). Despite numerous epidemiological studies, the mechanism of pipetting related MSDs in the hand has not been systematically explored.

Few researchers have quantified the force applied to the pipette or musculoskeletal loading while pipetting. Fredriksson (1995) assessed the push forces at the thumb required to operate a pipette and compared them with the participants' thumb strength. She found that the peak push force in operating the pipette is 18.4% and 14.5% of the push force capacity for female and male subjects, respectively. A more extensive biomechanical analysis was performed by Asundi et al. (2005) who evaluated the thumb push force and activities in four extrinsic muscles for different pipetting tasks. They found that high-precision tasks significantly increased static muscle activity but reduced peak thumb force on average 5% as compared with low-precision tasks; in addition, pipetting high-viscosity fluids increased peak thumb forces on average 11% as compared with pipetting low-viscosity fluids. The force magnitude and excursion of muscles/tendons of the thumb during pipetting have not been evaluated.

In order to elucidate the mechanisms of the MSD initiation and development in the hand related to pipetting, one has to know the muscle forces during the task. The purpose of the current study was to analyze the loading in the muscle–tendon units in the thumb during pipetting, accomplished via an inverse dynamic approach combined with an optimization procedure.

2. Methods

2.1. Experimental design

The test-setup in the study is similar to that used in our previous study (Wu et al., 2012). The pipetting tests were performed using a typical thumb-activated pipette (P200, Pipetman, Gilson, Inc, Middleton, WI, USA), which is actuated by a thumb-push button (Fig. 1A). The pipette has an adjustable dispensing capacity from 50 to 200 μl; and it was set at 150 μl during the tests. The plunger can be depressed fully in two stages; the stiffness of the spring mechanism for the first stage is much smaller than that for the second stage. The plunger press force was measured using a miniature force sensor (Series LBS-111 N, Interface Inc., Scottsdale, Arizona, USA) that was placed under the plunger button. The load cell is one-dimensional and it records only the axial force. Lateral forces on the push button, which may occur in inappropriate operation, are not considered.

2.2. Kinematics of pipetting

Kinematics for the thumb, fingers, hand, and forearm were determined using methods similar to those in previous studies (Sinsel et al., 2010; Buczek et al., 2011). Briefly, semi-spherical, retro-reflective markers (4 mm diameter) were applied individually on the finger/thumb/hand segments and pipette using a thin self-adhesive tape (Fig. 1B). The relative displacement of the plunger button was measured via two motion capture markers placed on the plunger press button and the pipette handle. The measurement model consists of 12 finger segments (three segments for each of the four fingers), three thumb segments, a hand, and a forearm. A total of 55 tracking motion markers were applied to obtain the pipetting kinematics. A 14-camera Vicon Nexus system (Oxford Metrics Ltd., Oxford England) was used to capture the motion marker trajectories at 100 Hz; the system has been calibrated in a control volume of approximately 3×3×2 (m) with a residual of less than 0.5 mm.

2.3. Multi-body dynamic model of pipetting

The hand is modeled as a multi-body linkage system and includes four fingers (index, long, ring, and little finger), thumb, and a palm segment (Fig. 2A). Each of the fingers is comprised of a distal, intermediate, and proximal phalanx, and a metacarpal. The thumb is comprised of a distal and proximal phalanx, a metacarpal bone, and a trapezium. The metacarpals of the four fingers and the trapezium of the thumb are considered to be fixed to the palm segment. Consequently, the palm segment includes the scaphoid, lunate, triquetrum, pisiform, hamate, capitate, trapezoid, trapezium, and four finger metacarpals. The four bones of each finger were connected by three joints: distal interphalangeal (DIP), proximal interphalangeal (PIP), and metacarpophalangeal (MCP). The DIP and PIP joints were modeled as hinges with one degree of freedom (DOF) (flexion/extension), whereas the MCP joint was modeled as a universal joint with two DOFs (adduction/abduction and flexion/extension). The four bony sections of the thumb are linked via interphalangeal (IP), metacarpophalangeal (MP), and carpometacarpal (CMC) joints. The IP joint is modeled as a hinge with one DOF (flexion/extension), the MP is modeled as a universal joint with two DOFs (adduction/abduction and flexion/extension), and CMC joint is modeled as a spherical joint with three DOFs (internal/external rotation, adduction/abduction, and flexion/extension).

Since the current study is focused on the thumb, the model includes only nine muscles that are attached to the thumb via tendons: flexor pollicis longus (FPL), extensor pollicis longus (EPL), extensor pollicis brevis (EPB), abductor pollicis longus (APL), flexor pollicis brevis (FPB), abductor pollicis brevis (APB), the transverse head of the adductor pollicis (ADPt), the oblique head of the adductor pollicis (ADPo), and opponens pollicis (OPP). The terminology describing the muscles is adapted from Smutz et al. (1998). The OPP and ADPt tendons will have variable wide, flat cross sectional areas and will be attached to bony sections via a narrow flat region rather than a point. These two tendons cannot be adequately represented using a single cord. In the proposed model, the OPP and ADPt tendons are modeled using three and four cords, respectively. The excursions in the OPP or ADPt tendons are evaluated using the averaged excursions of the multiple tendon cords; whereas the forces in these two tendons are evaluated by the sum of the forces in the multiple tendon cords.

The hand model was developed on the platform of the commercial software package AnyBody (version 5.0; AnyBody Technology, Aalborg, Denmark). A Hill-type, three-element model (AnyMuscleModel3E) was applied to model all nine thumb muscles. The three-element muscle model (van den Bogert et al., 1998) consists of a contractile element, an elastic element in parallel with the contractile element, and a serial elastic element. The effects of the force–velocity relationship, isometric force–length relationship, ratio of fast to slow fibers, and the pennation angle have been considered in the three-element muscle model.

The physiological cross-sectional areas (PCSAs), fiber lengths, and pennation angles of the muscles are adopted from the literature (Linscheid et al., 1991; Brand et al., 1981) (Table 1). The maximal isometric muscle force is calculated by multiplying PCSA by a proportional factor 35 N/cm^2. The ratio of the fast to slow twitch was assumed to be 0.4:0.6 for all muscles. The muscle–tendon attachment locations and other details of the thumb model have been described in a previous study (Wu et al., 2009). The 3D bony meshes were obtained commercially (TurboSquid, New Orleans, LA); they were scanned from a plastic skeletal hand model. The 3D mesh of the pipette was created using SolidWorks (Dassault Systemes SolidWorks Corp., MA, USA). The lengths of each bone mesh were scaled to fit the required phalanx lengths in the model.

2.4. Test protocol and analysis

Eight subjects (four male and four female; age 27.5 (2.6) years; body mass 89.2 (25.3) kg; height 170.1 (8.6) cm) participated in the study following informed consent approved by the local human subjects committee. All subjects were right-handed laboratory technicians who had more than two years of experience using pipettes, and use manual pipettes on a daily basis. The workbench was adjusted to a height similar to that in the laboratory environment. Subjects were instructed to extract the fluid from one container on their left side and dispense it to another container on their right side. Both containers were made of transparent Plexiglas and were identical in dimension (diameter 90 mm, height 24 mm). The containers were placed 120 mm apart center-to-center, which is typical in the work environment. The centers of the containers were marked and clearly visible to the subjects. Tap water stained light-brown using coffee was used as the pipetting fluid.

The subjects were instructed to pipette at a pace consistent with their routine use of pipettes, and to repeat the same procedure in the pipetting task: first press the plunger to the first stop, extract the sample fluid from the container by releasing the plunger, point the tip to a second container, and dispense the fluid by depressing the plunger to the second stop. The subjects were instructed to repeat the pipetting procedure throughout a 60 s session. No particular pipetting rate was set for the subjects. Before data collection, subjects had a chance to practice and become comfortable with the setup for about two minutes. To ensure greater consistency for each pipetting cycle, a custom-made audible pacer was set to match each subject's preferred pace, and this guided each subject during a pipetting session.

The recruitment of the muscle forces is calculated by using a min/max optimization procedure in AnyBody (Rasmussen et al., 2001), in which the maximal normalized muscle force is minimized under the constraints that the muscles are always in tension and the

dynamic force balance is maintained. Before the inverse dynamic calculations, the tendon lengths of the model are adjusted to minimize the passive muscle force and to make sure that all muscles work around their optimized muscle lengths during pipetting. The time-histories of each joint angle and the interface contact force between the thumb tip and the pipette's dispense plunger button were applied as input data, whereas the corresponding time-histories of the excursions and forces of muscle–tendon units of the thumb were predicted. The segments of each of the thumb and fingers were scaled independently to those measured from each of the subjects. When the bony dimensions are scaled, the muscle inserting and pulley locations are also scaled proportionally. The data obtained from all subjects were then averaged and the standard deviations were calculated.

3. Results

The calculated peak muscle forces of one subject were found to be more than (+/−) 2.0 SDs from the means of the other seven subjects for four muscles (APB, OPP, FPL, and EPB). Therefore, this particular subject was considered to be not representative for average pipette users and the corresponding results have been excluded from the following analysis.

Representative time histories of the push force and displacement of the plunger button are shown in Fig. 3A and B, respectively. The entire time duration for a pipetting task is divided into extraction and dispensing cycles, during which the pipette plunger moves a distance of 12 mm and 18 mm, respectively. The peak push force measured at the plunger button for the dispensing cycle is typically 2.5–3.0 times that for the extraction cycle (Fig. 3A). The average time period for the extraction and dispensing cycles is 1.87 (0.58) s and 1.71 (0.62) s, respectively.

Because the pipetting rate differed among subjects, ensemble average data were plotted against the percent of an extraction or dispensing cycle, as researchers traditionally do with gait analysis (e.g., Winter, 2005; Whittle, 2007). A working cycle is normalized in a range of 0–100%. The plunger push force and displacement as a function of the task cycle for seven subjects are plotted in Fig. 4. The left and right columns of Fig. 4 show the extraction and dispensing cycles, respectively. Despite variations in the magnitudes of the displacement and force among subjects, the patterns of displacement and force during the pipetting cycles were consistent: maximum displacement and force occurred near 50% of the extraction cycle, and near 75% of the dispensing cycle. The mean peak force for the dispensing cycle reaches 28 N, about 3.2 times that for the extracting cycle.

The muscle forces as a function of working cycles for APB, APL, and OPP are shown in Fig. 5; those in EPL, FPL, and ADPo are shown in Fig. 6; and those in ADPt, FPB, and FPB are shown in Fig. 7. The left and right columns of the figures show the extraction and dispensing cycles, respectively. The maximal muscle force was found in APB (Fig. 5); the mean peak value reaches 68 N during the dispensing cycle, approximately 2.3 times that of the peak push force. The maximal peak forces for all nine muscles are evaluated and compared with the corresponding maximal isometric forces (Table 2).

Despite differences in the force magnitude among the subjects, the general pattern of muscle forces for the working cycles are consistent. The muscle forces in APB, OPP, EPL, FPL,

ADPo, ADPt, and FPB reach their peaks around 50% and 75% for the extracting and dispensing cycle, respectively, which is approximately synchronized with the push force. The muscle activations in APL and EPB are a little different from all other muscles; the muscles are active only at the start and end of the cycle for extracting, whereas their activation patterns are similar to other muscles for dispensing.

4. Discussion and conclusion

Despite studies associating repetitive pipetting tasks with MSDs in the upper limbs (Baker and Cooper, 1998; Heath, 1998), musculoskeletal forces in the thumb during pipetting have not been analyzed. In the current study, we performed a detailed biomechanical analysis of the musculoskeletal loading in the thumb associated with pipetting. The proposed biomechanical model makes it possible to estimate musculoskeletal loading during pipetting, thereby contributing to elucidating the mechanism of the MSD.

The pipetting task is performed in a posture in which the thumb muscles generate force to stabilize the grip around the pipette and to press the plunger button (Johanson et al., 2001). The forces in APB and FPB were found to be substantially greater than those in other muscles. The muscle loading conditions in our case are similar to those observed in unstable pinch tasks (Johanson et al., 2001).

The previous kinematic analysis (Wu et al., 2012) showed that the pipetting action is realized mainly by the joint motions of IP in flexion, MP in adduction/extension, and CMC in abduction/extension, In comparison with the muscle–tendon moment potentials (Kaufman et al., 1999; Smutz et al., 1998; Wu et al., 2009), one would speculate that the joint motions during pipetting may be mainly generated by muscles FPL, EPL, and EPB/APL, which have large moment potential of IP in flexion, MP in adduction/extension, and CMC in abduction/extension, respectively. The forces in all other muscles may be required to keep the joints in balance mechanically.

It is interesting to note that the force cycle-histories of APB (Fig. 5A) and APL (Fig. 5B) are quite different in trends, although both of the muscles are located on the radial side of the thumb (Yu et al., 2004). The APB inserts on the proximal phalanx and passes across both MP and CMC joints; and the APL inserts on the metacarpal bone and passes across the CMC joint. The joint motion of MP during pipetting will have a direct effect on the APB, whereas it has no effect on the APL. The joint motion of CMC during pipetting will have an effect on APL and little effect on APB, because the magnitude of the muscle–tendon potential vector of the APL is about 2.5 times that of the APB in the muscle–tendon potential diagram of the CMC joint (Wu et al., 2009; Pearlman et al., 2004). In addition, the muscle–tendon potential vector of the APL is in an extension/abduction phase – the joint motion range in pipetting (Wu et al., 2012), whereas that of the APB is in a flexion/abduction phase. The force cycle of APB (Fig. 5A) and APL (Fig. 5B) is consistent in trend with the joint motion cycle of MP in adduction/abduction (Fig. 6A in Wu et al., 2012) and CMC in adduction/abduction (Fig. 7A in Wu et al., 2012), respectively.

Previous clinical observations indicated that development of carpal tunnel syndrome may cause weakness and early fatigue of APB (Kulick et al., 1986). It has been hypothesized that

the development of de Quervan's disease, a stenosing tenosynovitis of the first dorsal compartment of the wrist, is associated with repeated overstretching of EPB and APL tendons, causing accumulative injury to the gliding mechanism (e.g., Finkelstein, 1930; Keon-Cohen, 1951). This hypothesis has been supported by the Finkelstein's test (Finkelstein, 1930), a classic diagnostic test for de Quervain's disease, in which the EPB and APL tendons are stretched in a particular thumb/wrist position to reproduce the patient's pain (Kutsumi et al., 2005). In the pipetting task, about 70% of the pushing power was generated from the CMC joint (Wu et al., 2012) and the CMC motions were generated mainly by the EPB and APL. Our analysis indicated that the APB and APL generated considerable force during pipetting. The muscle forces in APB and FPB are quite large relative to all other muscles. In particular, the maximal muscle force during pipetting was found in APB, and the mean APB muscle force reached 68 N at the peak for the dispensing task (Fig. 5). In addition, the APB and FPB muscles have relatively small PCSAs (Table 1). Consequently, the relative forces or stresses in the APB and FPB muscles are the highest among all muscles (Table 2). Although we cannot conclude that pipetting task will cause carpal tunnel syndrome or de Quervain's disease in healthy workers, our results indicated that pipetting may be a difficult task or may make the symptoms worse if the operators already had carpal tunnel syndrome or de Quervain's disease.

The OPP muscle is the principal motion producer for the CMC joint in opposing/anteposition, which is in the range of motion for the CMC joint during pipetting. Because the OPP has a wide, flat cross-sectional area and is attached to the metacarpal bony section via a flat region rather than via a point (Fig. 2B), it plays an important role in maintaining the stability of the CMC joint, although the force in OPP is small compared to that in APB or FPB. Our results show that the mean peak force in OPP reaches 32 N, which is comparable to that observed in power grip (Kuo et al., 2009). Our results are qualitatively comparable to the EMG measurements by Valero-Cuevas et al. (2003) who found that OPP is the third most highly activated muscle, next to APB and FPB, during a power grip in an opposition posture.

The ratio of the mean peak muscle force (in APB) and the mean peak push force during pipetting is about 30% less than the corresponding values observed in grasping (Vigouroux et al., 2011), whereas the maximal muscle force is about three times more than that. However, the maximal muscle forces were found in different muscles in these two tests, because of the differences in postures. Because a force variation at the plunger push button will induce more than a doubled variation in the muscle forces, improving the pipette design to reduce the required button push force may greatly decrease the injury risk associated with pipette use, if muscle force is considered one of the major factors that cause MSDs in the hand.

The variations in the predicted muscles forces are observed to be substantial (Figs. 4–6), although the variations in the force and displacement at the fingertip are relatively small (Fig. 3). The variations in the muscle forces are mostly caused by the inter-subject variations in the postures and operation techniques. The same motion at the thumb-tip was observed to be realized by different individuals by using different joint kinematics (results not shown). For example, some subjects moved both their IP and MP joints during pipetting, whereas

some realized the same action by relying solely on their MP joint motion. Some subjects moved their IP joint in both extension and flexion, whereas others moved the IP joint only in flexion. Large variations in the ranges of the joint motions resulted in large variations in the predicted muscle forces. In addition, unskillful pipette users may apply quite a lot of lateral force on the push button and may have relative sliding of the pipette in the hand during pipetting; and these also contributed to the variations in the muscle forces.

In summary, we developed an inverse dynamic model to analyze the forces in muscle–tendon units of the thumb during pipetting. The time-histories of the forces in the muscle–tendon units during the extraction and dispensing cycles were calculated. The analysis method and results in the current study help to provide a mechanistic understanding of MSDs associated with pipetting, and may be useful in guiding ergonomic designs for manual pipettes.

References

Armstrong, T.; Fine, L.; Radwin, R.; Silverstein, B. Scandinavian Journal of Work, Environment and Health. 1987. Ergonomics and the effects of vibration in hand-intensive work; p. 286-289.

Asundi KR, Bach JM, Rempel DM. Thumb force and muscle loads are influenced by the design of a mechanical pipette and by pipetting tasks. Hum. Factors. 2005; 47(1):67–76. [PubMed: 15960087]

Baker P, Cooper C. Upper limb disorder due to manual pipetting. Occup. Med. (London). 1998; 48(2): 133–134. [PubMed: 9614772]

Barr AE, Barbe MF, Clark BD. Work-related musculoskeletal disorders of the hand and wrist: epidemiology, pathophysiology, and sensorimotor changes. J. Orthop. Sports Phys. Ther. 2004; 34(10):610–627. [PubMed: 15552707]

Brand PW, Beach RB, Thompson DE. Relative tension and potential excursion of muscles in the forearm and hand. J. Hand. Surg. (Am.). 1981; 6(3):209–219. [PubMed: 7240676]

Buczek FL, Sinsel EW, Gloekler DS, Wimer BM, Warren CM, Wu JZ. Kinematic performance of a six degree-of-freedom hand model (6DHand) for use in occupational biomechanics. J. Biomech. 2011; 44(9):1805–1809. [PubMed: 21530970]

David G, Buckle P. A questionnaire survey of the ergonomic problems associated with pipettes and their usage with specific reference to work-related upper limb disorders. Appl. Ergon. 1997; 28(4): 257–262. [PubMed: 9414365]

Finkelstein H. Stenosing tendovagnitis at the radial styloid process. J. Bone Joint Surg. 1930; (12): 509–540.

Fredriksson K. Laboratory work with automatic pipettes: a study on how pipetting affects the thumb. Ergonomics. 1995; 38(5):1067–1073. [PubMed: 7737101]

Heath CJ. Case report – upper limb pain attributed to repeated manual pipetting. Occup. Med. (London). 1998; 48(4):279–280. [PubMed: 9800428]

Johanson ME, Valero-Cuevas FJ, Hentz VR. Activation patterns of the thumb muscles during stable and unstable pinch tasks. J. Hand. Surg. Am. 2001; 26(4):698–705. [PubMed: 11466647]

Kaufman KR, An KN, Litchy WJ, Cooney WP, Chao EY. In-vivo function of the thumb muscles. Clin. Biomech. (Bristol, Avon). 1999; 14(2):141–150.

Keon-Cohen B. De quervain's disease. J. Bone Joint Surg. Br. 1951; 33-B(1):96–99. [PubMed: 14814168]

Kulick MI, Gordillo G, Javidi T, Kilgore ESJ, Newmayer WL. Long-term analysis of patients having surgical treatment for carpal tunnel syndrome. J. Hand. Surg. Am. 1986; 11(1):59–66. [PubMed: 3944445]

Kuo LC, Chang JH, Lin CF, Hsu HY, Ho KY, Su FC. Jar-opening challenges. Part II. Estimating the force-generating capacity of thumb muscles in healthy young adults during jar-opening tasks. Proc. Inst. Mech. Eng. H. 2009; 223(5):577–588. [PubMed: 19623911]

Kutsumi K, Amadio PC, Zhao C, Zobitz ME, Tanaka T, An KN. Finkelstein's test: a biomechanical analysis. J. Hand. Surg. Am. 2005; 30(1):130–135. [PubMed: 15680568]

Linscheid R, An KN, Gross R. Quantitative analysis of the intrinsic muscles of the hand. Clin. Anat. 1991; 4:265–284.

McKean ML, Costello K, Scordato R, Ligugnana R. Musculoskeletal diseases caused by use of micropipette in laboratory. G. Ital. Med. Lav. Ergon. 2005; 27(2):240–243. [PubMed: 16124538]

Muggleton JM, Allen R, Chappell PH. Hand and arm injuries associated with repetitive manual work in industry: a review of disorders, risk factors and preventive measures. Ergonomics. 1999; 42(5): 714–739. [PubMed: 10327893]

Pearlman JL, Roach SS, Valero-Cuevas FJ. The fundamental thumb-tip force vectors produced by the muscles of the thumb. J. Orthop Res. 2004; 22(2):306–312. [PubMed: 15013089]

Ranney D, Wells R, Moore A. Upper limb musculoskeletal disorders in highly repetitive industries: precise anatomical physical findings. Ergonomics. 1995; 38(7):1408–1423. [PubMed: 7635130]

Rasmussen J, Damsgaard M, Voigt M. Muscle recruitment by the min/max criterion – a comparative numerical study. J. Biomech. 2001; 34(3):409–415. [PubMed: 11182135]

Sinsel, EW.; Gloekler, DS.; Wimer, BM.; Warren, CM.; Wu, JZ.; Buczek, FL. A novel technique quantifying phalangeal interface pressures at the hand-handle interface. The 34th Annual Meeting of the American Society of Biomechanics (ASB-2010); Providence, RI, USA. 2010.

Smutz WP, Kongsayreepong A, Hughes RE, Niebur G, Cooney WP, An KN. Mechanical advantage of the thumb muscles. J. Biomech. 1998; 31(6):565–570. [PubMed: 9755041]

Valero-Cuevas FJ, Johanson ME, Towles JD. Towards a realistic biomechanical model of the thumb: the choice of kinematic description may be more critical than the solution method or the variability/uncertainty of musculoskeletal parameters. J. Biomech. 2003; 36(7):1019–1030. [PubMed: 12757811]

van den Bogert AJ, Gerritsen KG, Cole GK. Human muscle modelling from a user's perspective. J. Electromyogr. Kinesiol. 1998; 8(2):119–124. [PubMed: 9680952]

Vigouroux L, Domalain M, Berton E. Effect of object width on muscle and joint forces during thumb-index finger grasping. J. Appl. Biomech. 2011; 27(3):173–180. [PubMed: 21844605]

Wainstein JL, Nailor TE. Tendinitis and tendinosis of the elbow, wrist, and hands. Clin. Occup. Environ. Med. 2006; 5(2):299–322. vii. [PubMed: 16647650]

Whittle, MW. Gait Analysis: An Introduction. 4th edition. Butterworth-Heinemann-Elsevier; Edinburgh: 2007.

Winter, DA. Biomechanics and Motor Control of Human Movement. 3rd edition. John Wiley and Sons; Hoboken, New Jersey: 2005.

Wu JZ, An KN, Cutlip RG, Andrew ME, Dong RG. Modeling of the muscle/tendon excursions and moment arms in the thumb using the commercial software anybody. J. Biomech. 2009; 42(3):383–388. [PubMed: 19124127]

Wu JZ, Sinsel EW, Gloekler DS, Wimer BM, Zhao KD, An KN, Buczek FL. Inverse dynamic analysis of the biomechanics of the thumb while pipetting: a case study. Med. Eng. Phys. 2012; 34(6):693–701. [PubMed: 22015316]

Yu, H.; Chase, R.; Strauch, B. Atlas of Hand Anatomy and Clinical Implications. Mosby; St. Louis: 2004.

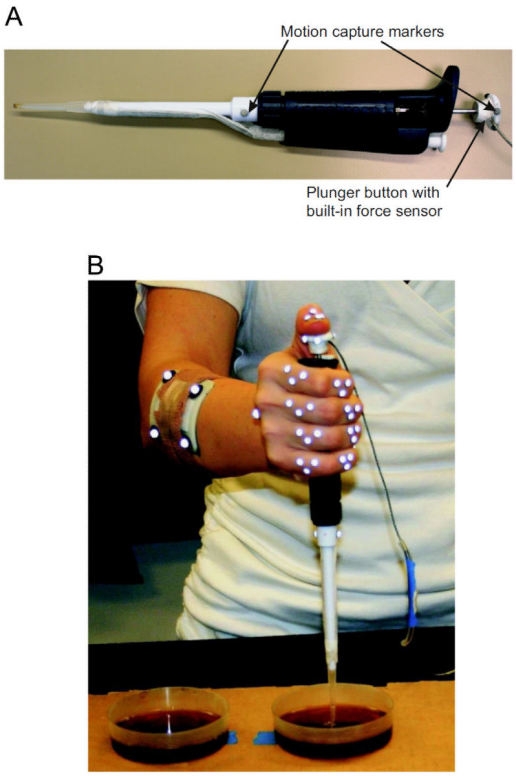

Fig. 1.
Experimental set-up. (A) The instrumented pipette used in the study. (B) The subject operating the pipette during the testing.

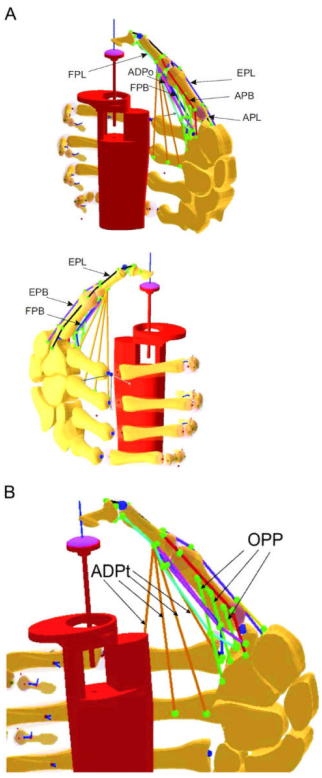

Fig. 2.

The model of pipetting. (A) Model of the entire hand with thumb containing detailed muscle-tendon connections. (B) Structure of ADPt and OPP muscles. The ADPt and OPP muscles are modeled with four and three strings, respectively.

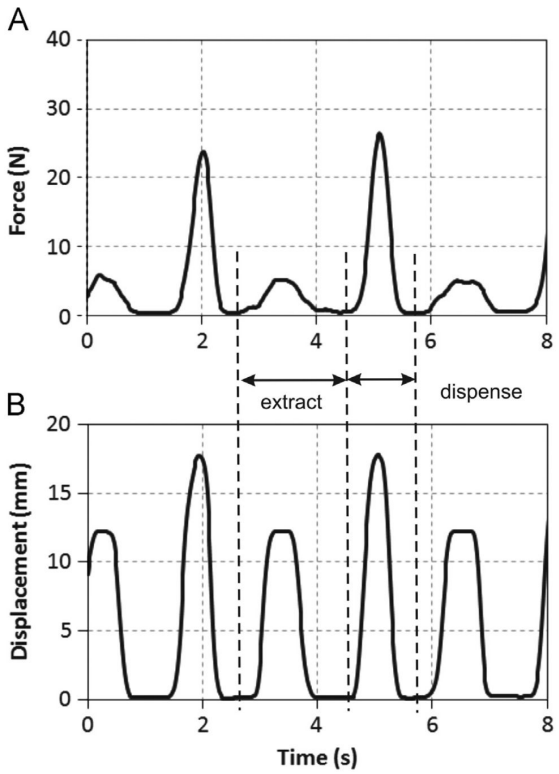

Fig. 3.

Representative time-histories of the displacement and force measured at the plunger button of the pipette. (A) Button push force. (B) Button displacement. The two neighboring peaks in the time-histories of the button displacement and push force represent the extraction and dispensing actions.

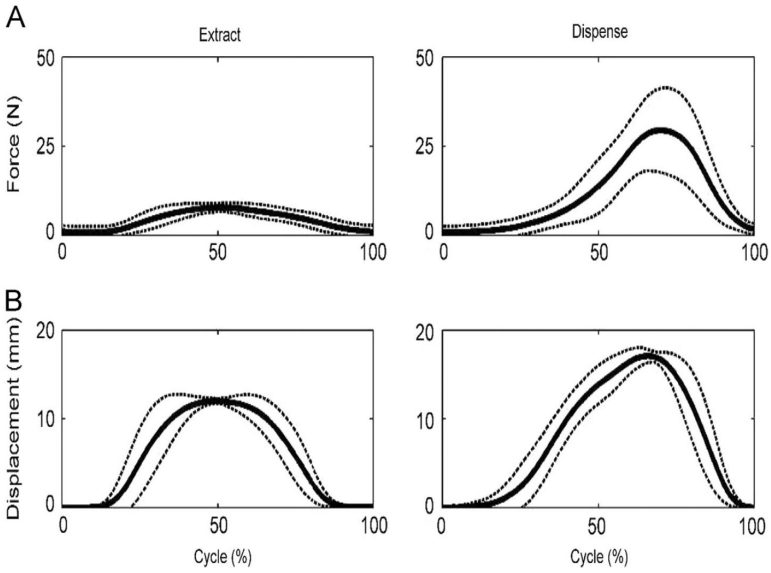

Fig. 4.

Variation in the push force and button displacement during the extraction and dispensing cycles. (A) The push force as a function of pipetting cycle. (B) The button displacement as a function of pipetting cycle. The solid lines represent the mean values of all eight subjects' data and the dotted lines are the standard deviations.

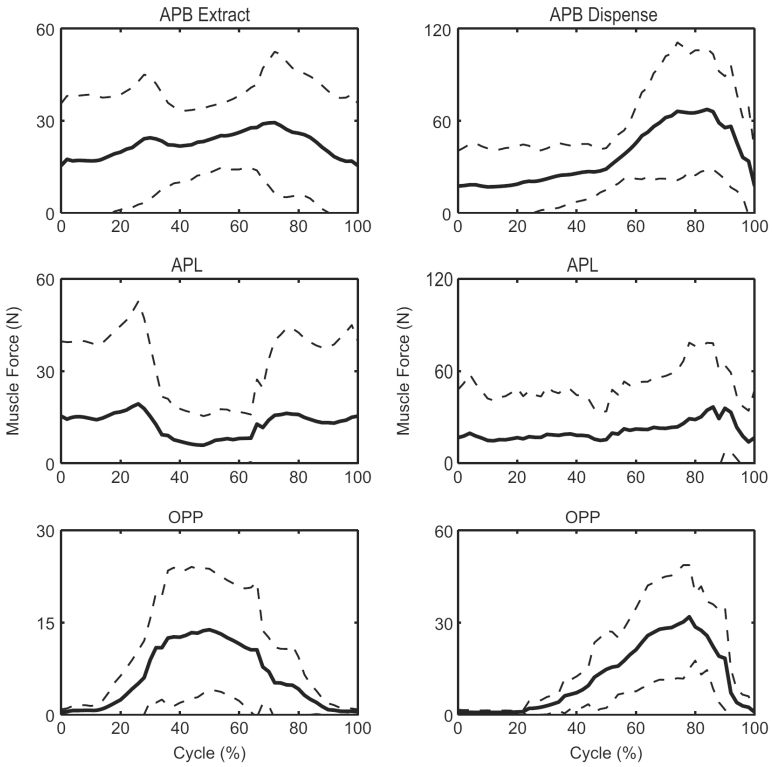

Fig. 5.

Variations of the APB, APL, and OPP muscle forces during the extraction and dispensing cycles. Left column: extraction. Right column: dispensing. The solid lines represent the mean values of seven subjects' data and the dotted lines are the standard deviations.

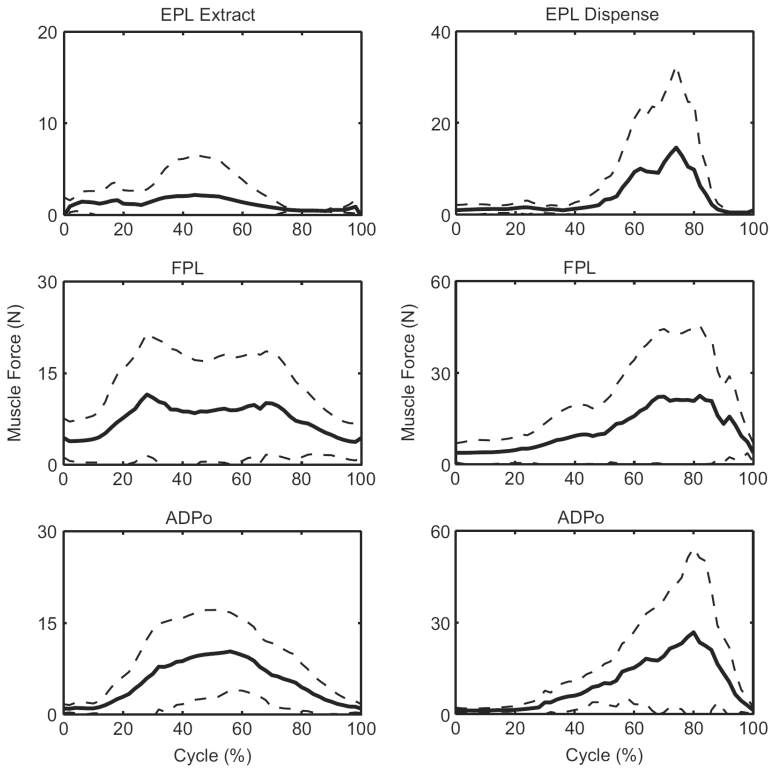

Fig. 6.

Variations of the EPL, FPL, and ADPo muscle forces during the extraction and dispensing cycles. Left column: extraction. Right column: dispensing. The solid lines represent the mean values of seven subjects' data and the dotted lines are the standard deviations.

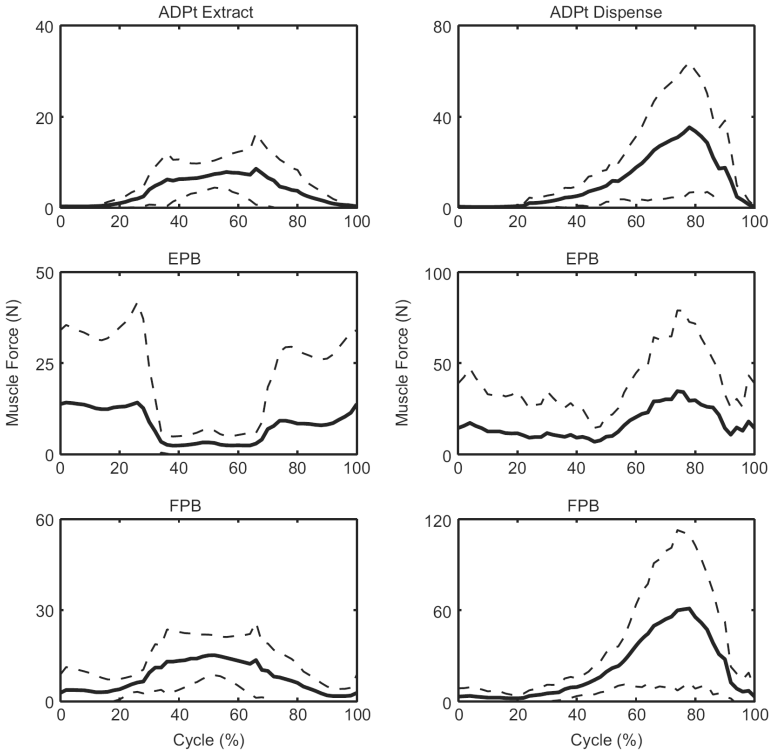

Fig. 7.

Variations of the ADPt, EPB, and FPB muscle forces during the extraction and dispensing cycles. Left column: extraction. Right column: dispensing. The solid lines represent the mean values of seven subjects' data and the dotted lines are the standard deviations.

Table 1

Physiological cross-sectional areas (PCSA), initial fiber lengths, and pennation angles of the thumb muscles at the un-deformed state.

Muscles	**APB**	**APL**	**OPP**	**EPL**	**FPL**	**ADPo**	**ADPt**	**EPB**	**FPB**
PCSA (cm^2)	1.5	3.9	2.8	1.9	5.1	1.3	0.9	1.3	1.3
Fiber length (m)	0.037	0.046	0.024	0.057	0.059	0.030	0.036	0.043	0.036
Pennation angle (°)	12.5	12.5	12.5	10.4	7.9	9.3	9.3	13.4	8.2

Table 2

Maximal isometric force, peak force, and loading intensity of the thumb muscles. The maximal isometric muscle force, F_0, is calculated by multiplying PCSA by a proportional factor 35 N/cm^2.

Muscles	**APB**	**APL**	**OPP**	**EPL**	**FPL**	**ADPo**	**ADPt**	**EPB**	**FPB**
Maximal isometric force, F_0 (N)	53	137	98	67	179	46	32	46	46
Peak force, F_m (N)	68	37	32	15	22	28	36	36	60
Loading intensity, F_m/F_0	1.30	0.27	0.33	0.23	0.12	0.62	1.14	0.79	1.32